Fabrication and mechanical properties evaluation of NbC-Ni cermets reinforced with B₄C and ZrB₂

Author

Maryam Saghir

2018-NUST-MS-DME-00000278121

Supervisor

Dr. Malik Adeel Umer

DEPARTMENT OF DESIGN AND MUFACTURING ENGINEERING

SCHOOL OF MECHANICAL & MANUFACTURING ENGINEERING

NATIONAL UNIVERSITY OF SCIENCES AND TECHNOLOGY

ISLAMABAD

September, 2021

Fabrication and mechanical properties evaluation of NbC-Ni cermets reinforced with B_4C and ZrB_2

Author

Maryam Saghir

Registration Number

00000278121

A thesis submitted in partial fulfillment of the requirements for the degree of

MS Design and Manufacturing Engineering

Thesis Supervisor:

Dr. Malik Adeel Umer

Thesis Supervisor's Signature: _____

Co-Supervisor:

Dr. Najam ul Qadir

Co-Supervisor's Signature: _____

DEPARTMENT OF DESIGN AND MUFACTURING ENGINEERING

SCHOOL OF MECHANICAL & MANUFACTURING ENGINEERING

NATIONAL UNIVERSITY OF SCIENCES AND TECHNOLOGY,

ISLAMABAD

September, 2021

THESIS ACCEPTANCE CERTIFICATE

Certified that final copy of MS/MPhil thesis Written by Maryam Saghir (Registration No: 00000278121), of SMME (School of Mechanical and Manufacturing Engineering) has been vetted by undersigned, found complete is all respects as per NUST Statutes/ Regulations, is free of plagiarism, errors and mistakes and is accepted as partial fulfillment for award of MS/MPhil Degree. It is further certified that necessary amendments as pointed out by GEC members have also been incorporated in this dissertation.

Signature: _____

Name of the supervisor: Dr. Malik Adeel Umer

Dated: __14-09-2021_____

Signature (HOD): _____

Dated: _____

Signature (Principal): _____

Dated: _____

i

Declaration

I certify that this research work titled "*Fabrication and mechanical properties evaluation of NbC-Ni cermets reinforced with B_4C and ZrB_2*" is my own work. This work has not been presented elsewhere for assessment. The material from other sources has been correctly acknowledged / referred.

Signature of Student

Maryam Saghir
00000278121

Plagiarism Certificate (Turnitin Report)

It is certified that MS/M.Phil Thesis Titled "**Fabrication and mechanical properties evaluation of NbC-Ni cermets reinforced with B$_4$C and ZrB$_2$**" by Maryam Saghir has been checked for Plagiarism. Turnitin report endorsed by Supervisor is attached

_____

Signature of Student

Maryam Saghir

2018-NUST-MS-DME-00000278121

_____

Signature of Supervisor

Dr. Malik Adeel Umer

Copyright Statement

Acknowledgements

First and foremost, I would like to show are gratitude to Allah Almighty who helped us in conducting this project. I am thankful to my parents and family for their endless love and support to reach the goals of my live.

I am grateful to my supervisor Dr. Malik Adeel Umer and my co-supervisor Dr. Najam ul Qadir for their countless efforts and guidance throughout this project and putting their confidence in me. Their comments, suggestions and questions were beneficial throughout in my project.

I would like to thanks Dr. Shamraiz Ahmad, Dr. Mushtaq Khan and Dr. Mohammad Khwaja for being on my thesis guidance.

I would also like to thank all the lab staff for their help in conducting experiments and testing in their respective labs. And special thanks to my friends for their endless support.

Dedicated to my exceptional parents, adored siblings and my beloved husband whose tremendous support and cooperation led me to this wonderful accomplishment.

Abstract

NbC-Ni cermet are a possible candidate for replacing WC-Co cermet cutting tools. It also overcomes the shortcomings of WC-Co tools. To study the fabricability of NbC-Ni cermets, firstly cermets with 8, 10 and 12 wt. % of Ni were fabricated and analyzed. Among these 12wt % Ni (NbC12Ni) cermet demonstrated an ideal combination of properties with the hardness of 1028 H_v, a flexural strength of 547.140 N/mm^2, a fracture toughness of 11.28 MPa $m^{1/2}$ and 99.5% densification. Further to have a better combination of hardness and strength addition of 2 wt. % B_4C (>5 um), 2 wt. % B_4C (3 um), and 5 wt. % ZrB_2 reinforcements in NbC12Ni system were studied. 2 wt. % B_4C (3 um) reinforced NbC12Ni (NbC12Ni2B_4C) exhibited the maximum hardness of 1235 Hv and a flexural strength of 506.217 N/mm^2 with 93.2% densification. Moreover, to improve the sinterability Ti was added and holding time was varied. Increase in holding time improved the densification in both B_4C and ZrB_2 system, whereas Ti added only in B_4C system (NbC12Ni1.2Ti2B_4C) resulted in drastic improvement in the densification and demonstrated the maximum hardness of 1390.6 Hv and a flexural strength of 506.138 N/mm^2 with 96.8% densification.

Key Words: *Liquid phase sintering, microstructure, densification, hardness, flexural strength*

Table of Contents

List of Figures

List of Tables

CHAPTER 1: INTRODUCTION

1.1   History of Cutting tools

Cutting tools has a history of over a century. Cutting tool materials have been enhanced to respond to certain requirements, needs, and problems that arose with the period of time. Consistent efforts have been put since 1900s to improve the material properties for cutting along with lifetime upgradation of the cutting tools. In early 1900, first high-speed steel was made available in market. [1]

Cemented carbide was invented in 1923. Apart from WC, other hard materials i.e., carbides were developed. TaC-Ni alloys were sold in US market with tradename Ramet. Other alloys such as $TiC-Mo_2C-Ni-Cr$ were developed and commercialized in Austria. These alloys were given a tradename of Titanit. Hindrance in the use of these alloys were lower toughness as compared to cemented carbide. Cermets had been in consideration since World War II. After this war, research and development was actively promoted. In 1950, this research resulted in the development of various cermets with useful toughness and hardness properties. [2]

Use of cermet for cutting tool inserts have found a very keen interests from the beginning of cutting tools history. In the category of cermet, cemented carbide was the material that took a great attention of researchers. It was first developed by the company Osram Lamp works having tradename 'WIDIA' by Krupp AG, Germany. It was a renowned success that cemented carbide can achieve the steel cutting speeds of 100 to 150 meter per minute. This was approximately four times higher speed than that of high-speed steel that has a cutting speed of 20 to 40 meter per minute. In the year 1928, Sumitomo Electric Industries Ltd. successfully launched a wire drawing die made of cemented carbide [3]. This was the foremost Igetalloy product ever in history. In 1931, cemented carbide cutting tool was commercialized by same company. The cutting tools has been shown in figure below:

Figure 1.1: Cemented Carbide Cutting Tools [3]

Since then, cutting tools materials had been in research for improving performance and meet the customer demands. Research on titanium carbide TiC started after 1932. It shown an increased lifetime was associated with crater wear. Crater wear resistance can be attributed to the scratching of rake face using chips. Therefore, it was a challenge for the researchers to enhance the lifetime of cutting tools at that time. TiC addition to cemented carbide had shown remarkable properties for the increase in lifetime of cutting tools. In 1936, first TiC added cemented carbide was commercialized. [1]

In order to meet the diversifying user needs in the years of 1930, different researches had been made to develop the properties of cutting tool materials. Additional cemented carbide types had been introduced. Four grades of cermets were developed namely S1, S2, G1, and G2. First two were used for cutting tools required to machine steel while the later two for cast iron. In 1965, these four materials resulted in the development of 26 different type of cermets to be used as cutting tool inserts. The addition of wide variety of cutting tools was immense and wondering but it added a problem to the customer's choice. Because people started confusing for what material they shall choose. Therefore, it emerged a need to develop the cutting tool materials that are suitable for wide range of materials. This research resulted in G10E material that was made to cut cast iron. This grade was made with WC-Co. It is still in use current market due to ease of manufacturing and mature technology. [3]

Further research continued to unify materials for steel cutting tool materials, cast iron cutting tool materials and etc. For steel cutting tool materials, ST20E was proposed in 1966. For

this material, the researchers have to tackle the two conflicting properties i.e., wear resistance and chipping resistance. Wear resistance also include crater wear resistance. For this, two grades P10 and P20 materials served the purpose of baseline criteria for ST20E. A compromise between these two properties had been investigated by adding different carbide, nitride, and oxide based cermets. An alloy structure named ST20E was made in order to serve as the compatible solution for wear and chipping resistance. This alloy structure comprised of complex carbonitride with metals like Ta, Ti, and W along with refined WC particle size. WC was present as a main hard phase in refined carbonitride matrix. Increasing the percentage of hard phase was the solution to find compromised properties.

In 1976, another material named AC720 was launched with higher wear resistance due to presence of TiC coating. This material was mainly used for cutting tool including steel turning applications. In the upcoming years, Sumitomo Electric worked for the development of nitrogen containing cemented carbide with commercial name A30N. This material was offered for milling cutter material. In 1984, nitrogen containing compound such as TiWTaCN was added to WC with refinement and dispersion of hard nitrogen component. This material was tested for compatible chipping and wear resistance properties. In 1994, Zr added substrate was developed to be used as cutting tool material for steel turning. This material was named AC2000. In those years, there was an increased need of higher speeds as well as higher feed rates for steel turning applications. In the latter half of the 1970s, cemented carbide tools coated with alumina or titanium compound were developed. They have much higher cutting speeds. WC-Co was developed actively for about a century. These light weight cermet materials have shown progress to be used as cutting tools.[1]

Majority of cutting tools make use of cemented carbide in the present era. It is due to higher speed of cutting tools as compared to high-speed steel cutting tools. Figure 1.2 shows the advancement and progress of cutting tool materials in the previous centuries. [3]

3
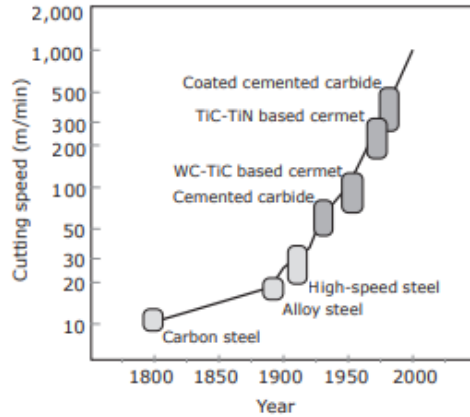
Figure 1.2: Progress of Materials for High Speed [3]

1.2   Cermet

Cermet is a term that is used to describe the engineered composite made by two different phases, namely ceramics and metals. In this composite, metal acts as a binder phase while the ceramics act as reinforcement phase. If we consider the ceramic phase, it includes a number of compounds such as carbides, nitrides, carbonitrides, and oxides of different metals including titanium, tungsten, niobium, molybdenum, tantalum etc. Carbides and nitrides of nickel, molybdenum, and cobalt alloys have also been used as a ceramic reinforcement in cermet. Metal binders include nickel, iron, cobalt, molybdenum and various alloys [4].

Cermets possess high hardness due to presence of ceramic reinforcement phase while giving a better toughness property due to metallic phase. These properties render the application of cermets in various categories such as slurry nozzles, bearings, coatings for corrosion and erosion protection, cutting tools, and many more. It is mainly due to excellent mechanical properties of cermet with a very high wear resistance. Moreover, ceramic phase provides a good oxidation resistance to overall cermet material. These properties make their use important for ballistic impact protection also. Better oxidation resistance attributes the application of cermet for metal machining and edge build up formation due to increased high temperature hardness and chemical stability [5].

4

In 1927, the first generation of cermet with Tungsten Carbide (Ceramic) and Cobalt (Metal) emerged. After WC-Co, various other compounds such as TiC and titanium carbide or nitride with metal binders such as Fe, Ni, Co, and Mo, have been developed to improve the properties of cermet [6]. Cermets are synthesized/prepared by milling, mixing and sintering of raw materials including carbides, oxides, and nitrides. Metal binders provide denser bodies when processed through liquid phase by sintering. Conventional cermets can deteriorate at very high cutting speeds and temperatures due to their lower chemical stability and plastic deformation.

1.2.1 Properties of Cermet

Cermets include advantages of both metal and ceramic phases i.e., low density, good wear resistance, high hardness, and better heat conductivity. Moreover, they will not undergo cracking mechanism at instant cooling or heating. Cermets can be used as a coating to prevent the oxidation and corrosion resistance during high temperature application of metals [7].

Application of cermets in cutting tool technology can be attributed to following properties:

1.2.1.1 Wettability of Ceramic to Metal Phase

The properties of cermet are dependent on the wettability of ceramic-metal interphase. It determines the microstructure and properties of cermet. If the wetting ability of metal with ceramic is higher, it will form a continuous phase. Thus, resulting in good cermet properties.

1.2.1.2 No Chemical Reaction

Reaction at interface of ceramic and metal determines the mechanical and thermal shock resistance. If the interfacial reactions occur, it will cause a hurdle in the preparation of cermet. Also, the ability of cermet to give resistance to thermal and mechanical shock will be reduced.

1.2.1.3 Slight Difference in Temperature Co-efficient

There is lesser difference in thermal co-efficient of ceramics and metals that results in the generation of very low internal stresses that increases the thermal stability of cermet.

5

1.2.1.4   Toughness Enhancement for Ceramics

Ceramic materials have the properties of high wear resistance, chemical stability, heat resistance, and high degree of hardness. But ceramic materials are very brittle that hinders their application at various places. Therefore, in order to lower their brittleness and add to their toughness value, different approaches have been used. Addition of metal causes an increase in toughness of cermet. Metal acts as an addition re-enforcing phase to enhance the fracture toughness of structural ceramics [8, 9].

1.2.1.5   Thermal Shock Resistance

Thermal shock behavior of cermets had been explained by using classic theory given by Hasselman in 1969. Classic theory explains the opposing property requirements whether the material is to be resistant to crack initiation with high strength and low stiffness or either shall provide resistance to degradation when applied a thermal shock. For thermal shock resistance application, low strength with high values of stiffness is required. So, the theory is based on opposing property requirements prevail. It describes whether the cermet is needed to be resistant after the initiation of cracks or either it shall provide strengthen degradation when several thermal shocks are applied [10].

1.2.2   Types of Cermet

Cermets consist of a ceramic matrix that is bonded by using a metallic binder. The presence of metal improves toughness of ceramic along with thermal shock resistance. Cermets consists of two major groups namely hard metals and oxide cermets. Hard metal cermets are made up of carbides, borides, nitrides and silicides of elements of Group IV to Group VI.

Hard metal cermets are usually carbides such as tungsten carbide with cobalt and nickel. Another cermet namely TiC-Co-Ni are in use for different applications e.g., cutting tools fabrication for various machines [11, 12]. Use of cermets for cutting tools application is attributed to compromise between hardness and toughness. It makes cermets to be used at commercial level for the fabrication of wear resistant components along with chemical

resistance. It makes cermets available to be used for high temperature applications as well as insulators. Each type is described below in detail:

1.2.2.1   Carbide Cermet

In this type of cermet, carbides are used as a particulate reinforcement in certain metal matrix. Commonly used carbide materials are titanium carbide, chromium carbide, and tungsten carbide. While the metal matrix is made up to either nickel or cobalt or an alloyed metal.

Cobalt has been specified for tungsten carbide by the researchers while nickel is recommended as a matrix material for carbides of titanium. If cermets are considered, generally the percentage of matrix material is very small as compared to particulate phase. This percentage is defined to be in the range 5 to 15%. If rupture strength of carbide cermet is to be increased, the percentage of metal matrix phase is increased and that of particulate phase is lowered. It causes a decrease in hardness but corresponding increase in rupture strength [13].

If we consider the application of carbide cermets, it has been seen in past that tungsten carbide is widely used for machining applications. The cutting tools, drill bits, hardness testing indenters, mining and rock drilling tools make an immense use of tungsten carbides cermets due to hardness and wear resistant properties as toughness is introduced by the presence of metal matrix.

Chromium carbide is known for its strong corrosion resistance properties and hence, chemical stability. If we compare it to the properties of other cermets, it has a much higher value of brittleness. Therefore, it finds application in bear seal rings, spray nozzles, vale liners and gage blocks [14].

Titanium carbides provides utmost applications for high temperature applications. Cermets with TiC use nickel as a matrix or binder. Mostly, gas turbine nozzles are made using titanium carbide cermets. It is because these cermets provide high temperature oxidation resistance making them reliable to serve the purpose [11].

One of the most widely used cermet is made up of tungsten carbide (WC) with metal matrix consisting of cobalt. The percentage of cobalt in this cermet is about 6%. WC–Co cermets give a toughness value of up to 10 to 15 MPa per square meter. This value is attributed towards the presence of cobalt that imparts ductility. WC-Co is used as an additional part incorporated on the surface of metal parts in various tools and machines to provide wear resistance [14].

1.2.2.2   Oxide Based Cermet

Aluminum oxide and magnesium oxide act as a particulate phase in oxide based cermets. Metal matrix in this case consists of chromium. Other metals such as nickel, cobalt can also be used a matrix or binder for specified applications. In order to variate the properties of these cermets, the ratio of particulate to matrix phase is changed. Oxide based cermets find application in cutting tools, mechanical seals, and thermocouple shields. There high temperature resistant properties make them suitable to be used as missile nozzle insert, melting metal crucible and cutting tool [15].

1.2.2.3   Nitride Based Cermet

The stability in aggressive media and metal vapors are the key features of nitride based cermets. They provide excellent chemical stability in chemically active environments along with wear and heat resistance. Nitride based cermets use metals from Group IV to VI. They have a property of rapid cutting and machining of steel and cast iron parts. Nitrides are prepared by using gas-phase reactions. These reactions involve precursors of transition metals and particulate nitrides. In addition to transition metals, metallic alloys are also used as a matrix for these cermets. The development of alloyed nitrides has emerged from titanium and zirconium nitrides. These cermets are then used as a coating to serve tool purposes [12].

1.3   Carbide Based Cermets

Carbide based cermets provide resistance to brittle fracture due to presence of carbide phase. This resistance is controlled by the level of elastic strain energy that has been transmitted to the surface of cutting tools. Moreover, it depends on the modulus of elasticity that is inversely

proportional to the elastic surface energy [16]. As the wear resistance of cermets depends on both fracture resistance and hardness, the carbide based cermets provide higher wear resistant properties as compared to nitride and oxide-based cermets. These materials include WC-WB-Co and WC-FeCrAl coated carbide based cermets along with low friction co-efficient [17]. To increase the wear resistance and hardness by increased densification, a low elastic modulus phase is added to oxide-carbide cermet system in which TiC is added to Al_2O_3. Small metal additions (such as Nb or Ni) can also be made with 3% by weight. Densification of the carbide phase can be achieved by spark plasma sintering [18].

Carbide based cermets provide lower value of free energy formation that makes them able to avoid crater wear. Crater wear is caused by the thermochemical reactions between insert and the chips. Carbide based cermets provide better crater resistance due to hard particles that resist diffusion of the cracks to tools rake face [19]. Moreover, the better toughness properties of carbide based cermets as compared to oxide and nitride based cermets. Stability of carbide phase minimizes crater wear resistance and chemical stability at higher temperature because it is less prone to oxidation. Cermet resist piling up at edge because of solubility of hard material (carbide) into iron. Low solubility of hard phase makes it difficult for the workpiece material to adhere to cutting edge of tool, thus making it suitable for cutting [20].

1.4   Liquid phase sintering

Liquid phase sintering (LPS) is a process to form components from powders having high performance and multiple-phase. LPS involves sintering under conditions where solid grains coexist with a wetting liquid. Different variants of LPS are applied to a wide range of engineering materials. Some examples for this technology are found in the applications of high-speed metal cutting inserts and automobile engine connecting rods.

1.4.1 History of LPS

Early uses of LPS required firing ceramics with a glass bond. The glass turned into a viscous liquid at high temperatures. In some ceramic compositions, the liquid phase is considered a viscous glass but we will refer to it as a liquid for this treatment and study.

In 1930s, the important technical advances in LPS came with the development of several materials such as cemented carbides (WC–Co), copper steels (Fe–Cu–C), tungsten heavy alloys (W Ni–Cu), porous bronze (Cu–Sn), and cermets (TiC-Fe). Over the period of next 70 years till 2000, LPS processing spread to a wide range of applications that includes porcelain jacketed dental crowns, wire drawing dies, oil well drilling tips, ultrasonic transducers, automotive valve seats, high-temperature bearings, electrical contacts, electronic capacitors, radiation shields, electronic solders, electronic insulator substrates, diesel engine turbochargers, golf clubs balance weights, and grinding abrasives.

1.4.2 Mechanism of LPS

In Figure 1.3, we have mentioned the conceptual view of the steps taking place for the case of two mixed powders. The solid grains undergo solid-state sintering during heating. Different microstructure evolution pathways are possible depending upon the solid–liquid solubility relation. Usually, the liquid to wet the solid but in this case, the newly formed liquid penetrates between the solid grains, dissolves the sinter bonds, and induces grain rearrangement. Furthermore, because of the solubility of solid in the liquid, the transport rates responsible for grain coarsening and densification are improved by the liquid. The surface energy linked with pores leads to their annihilation, while there is progressive microstructure coarsening and bonding to increase rigidity.
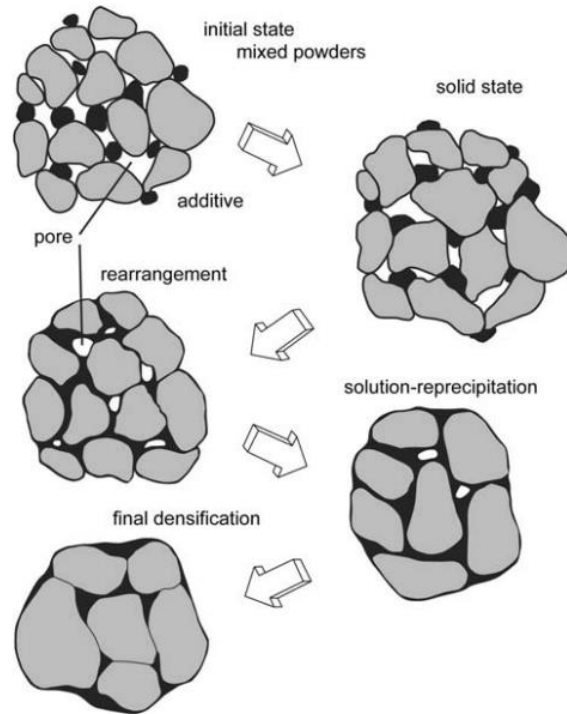
Figure 1.3: Schematic of Liquid Phase Sintering [21]

1.4.3   Wetting mechanism during LPS

When the liquid is formed in LPS, the microstructure consists of solid, liquid, and vapor. The liquid that is spread on the solid replaces solid–vapor interfaces with liquid–solid and liquid–vapor interfaces. Figure 1.4 contrasts good and poor wetting based on the contact angle.
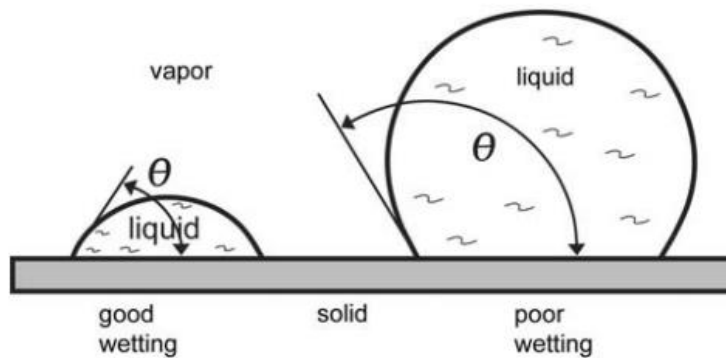
Figure 1.4: Wetting behavior of liquid on solid substrate [21]

A low-contact angle induces liquid spreading over the solid grains which provides a capillary attraction that helps in densifying the system. For small grains, contact stress can compete with that seen in pressure-assisted sintering techniques like hot isostatic pressing. In practice, since the microstructure is composed of a range of grain shapes, grain sizes, pore shapes, and pore sizes, a broad range of capillary conditions exists each with a different capillary condition. A wetting liquid preferentially flows to the smaller grains and pores as it moves to occupy the lowest energy configuration. This increases the rearrangement densification. Since heat flow from the furnace determines the rate of melt formation, and compacted powders are poor thermal conductors so rearrangement takes a few minutes. A high-contact angle indicates poor wetting, so the liquid retreats from the solid. This results in compact swelling and liquid exuding from pores. Thus, liquid formation causes either densification or swelling depending on the contact angle. The magnitude of the capillary effect depends on the amount of liquid, contact angle and particle size.

1.4.4   Solution re-precipitation during LPS

The first mechanism is the contact flattening. It is shown in Figure 1.5 (a). A compressive force at the grain contacts from the wetting liquid which pulls the grains together. This capillary stress results in the preferential dissolution of solid at the contact point with the re-precipitation at regions away from the contact. Densification is caused from the center-to-center motion of grains. The main step is the diffusion of solid in the liquid to the regions away from the contact zone. For small grains, the contact zone stresses are comparatively large, so contact flattening tends to dominate LPS. However, contact flattening does not explain the decrease in the number of grains and the grain growth. When grain growth is inhibited there is less grain shape accommodation.

The second mechanism of densification involves the dissolution of small grains with the re-precipitation on large grains. Small grains disappear while the large grains grow and undergo shape accommodation. The controlling transport mechanism in the liquid is diffusion, as shown in Figure 1.5 (b). The second mechanism does not involve shrinkage, so it is not an explanation

for densification, except that better packing of the solid is enabled due to the grain shape accommodation.
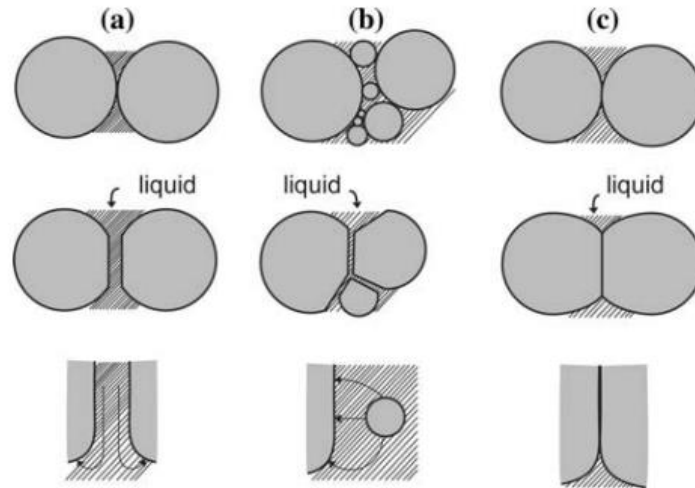
Figure 1.5: Mechanisms of grain shape and neck growth during LPS densification (a) contact flattening, (b) dissolution of small grains, and (c) solid state bonding [21]

The third mechanism requires the growth of the inter-grain contact by diffusion along the grain boundary of the wetted liquid, as it is shown in Figure 1.5 (c). The contact zone expands to change the shape of the grain with simultaneous shrinkage of the grains. This does not require the coarsening of grain. Instead, it includes a cooperative redistribution process of the mass deposited where the grain boundary intersects the liquid. These three mechanisms vary in the source of the solid and in the comprehensive transport path, but together they explain grain growth, grain shape accommodation, and densification. Grain growth takes place with densification. In fact, the grain size and density tends to follow a usual trajectory for most of the LPS systems. This shows more rapid grain growth as the pores are removed. Although the neck growth is active in the start, it is not enough to explain the changes of all microstructures. On the other hand, the small grain dissolution and contact flattening couple to completely explain the density progression and microstructure typical to LPS.

CHAPTER 2: LITERATURE SURVEY

This chapter discusses the motivation behind the selecting NbC and the ways to improve its mechanical and tribological properties. Figure 2.1 demonstrate a brief mind map which will be discussed in detail throughout this chapter.
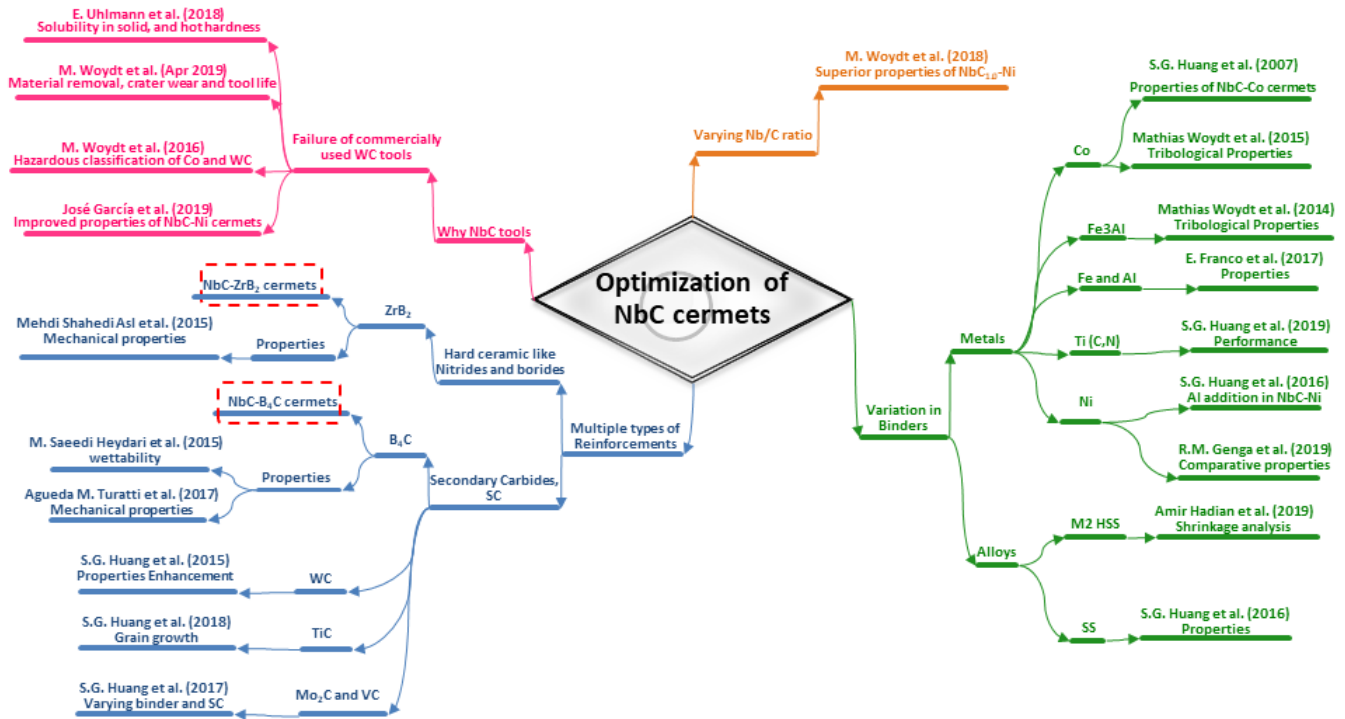
Figure 2.1: Mind map of literature available on NbC cermets

2.1 Why NbC Cermets – Drawbacks of WC cermets

2.1.1 Health hazards

Tungsten carbide and Cobalt metal have given way to a whole new spectrum of health issues and risks [22, 23], this involved progressively more severe tags. Up till now no restriction of critical classifications has been associated with bulk cobalt metal (Co), Tungsten Carbide (WC) and Niobium Carbide (NbC). However, during the cutting process high temperatures are

produced due to the cutting heat, this cause WC and Co to form their respective oxides that are Tungsten trioxide (WO_3) and tricobalt tetraoxide (Co_3O_4).

These oxides can be formed by oxidation, tribo-oxidation and also through the chemical reactions with the metal cutting fluids. These oxides are released to the environment either through aerosols salts or wear particles. Along with Co_3O_4 some other salts of cobalt metal are being classified in several concerns and labels in the framework of European organization REACH (stands for: Registration, Evaluation, Authorisation and Restriction of Chemical substances programme). The website of European Chemicals Agency (www.echa.europa.eu) does contain this organizations details.

The oxide of NbC produced during cutting is Niobium pentoxide (Nb_2O_5) which up to date have not received any concerned notification like H341, H350, H351 or H360 and this oxide is registered fully by REACH. Neither Nb_2O_5 nor NbC have been filed for any critical or hazards notification in the framework of REACH.

Health hazard classifications like mutagenic, carcinogenic, and toxic for reproduction are all summarized and mentioned in Table 2-1. Through this table it is clearly visible that Co_3O_4 can cause genetic disorder, cancer and can damage fertility. Whereas, WO_3 is also suspected to cause cancer and it is classified under H351.

Table 2-1: Health hazards overview of Co_3O_4, WO_3 and Nb_2O_5 [24]

Substance	Hazard class and classification code			
	Mutagenic category 2	Carcinogenic category 1A	Reproductive toxicity category 1B	Carcinogenic category 2
Co_2O_4	Yes (H341, suspected of causing genetic defects)	yes (H350, may cause cancer when inhaled)	Yes (H360, may damage fertility)	——
WO_3	——	——	——	yes (H351, suspected of causing cancer)
Nb_2O_6	——	——	——	——

15

In comparison with Cobalt metal powder, Nickel (Ni) metal powder does not demonstrate the similar harmful classification. That's why Ni bonded Niobium Carbide can be a feasible substitute to Co bonded Tungsten Carbide. If we look into the biocompatibility of metals, Niobium metal is one of the most biocompatible metal, and this extended to Niobium Carbide over an extensive variety of stoichiometry. This biocompatibility of NbC was assessed by means of cell viability tests as and was compared by implants used in human body i.e. Ti-6Al-4V alloy [25] and Nb_2O_5 [26].

2.1.2 Wear properties comparison

Figure 2.1 demonstrate that NbC tool is a potential candidate for machining of C45E carbon steel and 42CrMo4+QT which is a hardened, quenched and tempered steel and it can easily replace WC tool.

With the increase in cutting speed the mean material removal V_w of C45E work piece remain constant with $NbC_{0.88}$-12Co cutting insert, which exhibit an uninterrupted increase in the stability of the process. An elevated value of mean material removal V_w at all variations of cutting speed was observed for $(NbC_{1.0}$-10TiC)-6Ni7.5VC cutting inserts with similar trend as visualized with $NbC_{0.88}$-12Co cutting insert. Whereas material removal with WC-6Co cutting inserts decreases with cutting speed, and at minimum speed the material removal is in between both the other two inserts, but as the speed increases the material removal of this insert becomes the minimum.

Turning operation performed on 42CrMo4+QT demonstrate different results as compare to C45E carbon steel work piece. At slowest cutting speed (V_c) i.e. 70m/min, $NbC_{0.88}$-12Co cutting insert indicates a four times higher material removal V_w compared to WC-6Co tool. However, as the cutting speed increases to 100m/min and 150m/min potential remains unchanged with an average drop of 20 % and subsequent 30 % respectively in the material removal was seen.

16

Spontaneous tool failure at elevated cutting speeds $V_c = 100$ m/min and $V_c = 150$ m/min limits the overall process stability. At all cutting speeds (NbC1.0-TiC)-6Ni7.5VC cutting insert had the highest material removal rate, which makes it a suitable alternative for WC tool.
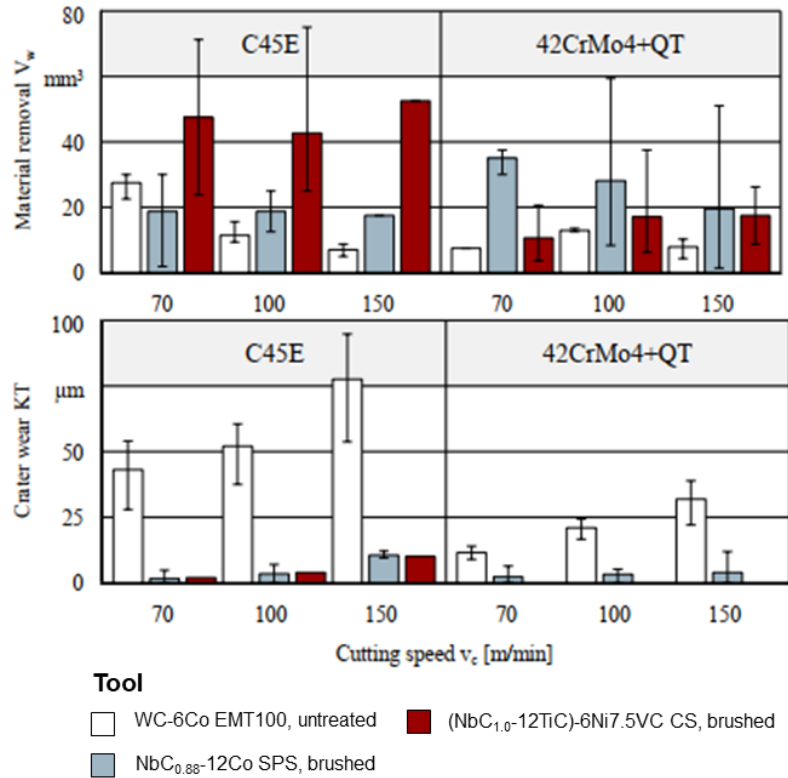
Figure 2.2: Results of machining of carbon steel with NbC and WC tools [27]

2.1.3   Solubility limit in different metals

Tools need high hardness and toughness, in order to control wear mechanism which may include adhesion, abrasion, tribo-mechanical wear and surface wear and tear in machining processes. Furthermore, to meet the conditions in high performance machining and ensure process stability, high mechanical strength along with thermal and chemical stability is needed. Because of a lesser solubility of binder less NbC in solid chrome (Cr), nickel (Ni), cobalt (Co) and iron (Fe) as compared to WC, a lessened chemical wear on the rake fake is expected. Due to the higher melting point of NbC with TM = 3520 °C along with a lower solubility in alloys,

adhesion with the workpiece during machining is reduced. Further advantageous properties that have been reported are, lesser wear rate caused due to the friction caused at elevated speeds and a higher hot hardness as of T ≈ 800 °C of sub-stoichiometric and stoichiometric NbC substrates as compared to WC-6Co. Keeping in mind the conditions in machining operations centered on thermomechanical loads, NbC exhibits the capacity as a cutting tool for a variety of steel based work piece materials.

Table 2-2: Solubility of metals in WC and NbC [27]

Metals	WC	NbC
Nickel	12	3
Cobalt	22	5
Iron	7	1
Solubility at T= 1250 °C [wt.-%]		

2.1.4 Hot hardness

Owing to a reduced solubility of binder less NbC in solid chrome (Cr), nickel (Ni), cobalt (Co) and iron (Fe) compared to WC, a lessened chemical wear on the rake fake is expected. Due to the higher melting point of NbC with TM = 3520 °C along with a lower solubility in alloys, adhesion with the work-piece while machining is reduced. Further advantageous properties that have been reported are, lesser wear rate caused due to the friction caused at elevated speeds and a higher hot hardness as of T ≈ 800 °C of sub-stoichiometric and stoichiometric NbC substrates as compared to WC-6Co.

2.2 Advancements in NbC Cermets

2.2.1 Nb/C ratio variation

Figure 2.3 demonstrate the binary phase diagram of Niobium (Nb) and Carbon (C), from this it can be visualized that other than NbC there are many cubic sub-carbides e.g. Nb_4C_3 or

Nb$_6$C$_5$ which can be formed at a long range of carbon stoichiometry, whereas WC does not show such feature.
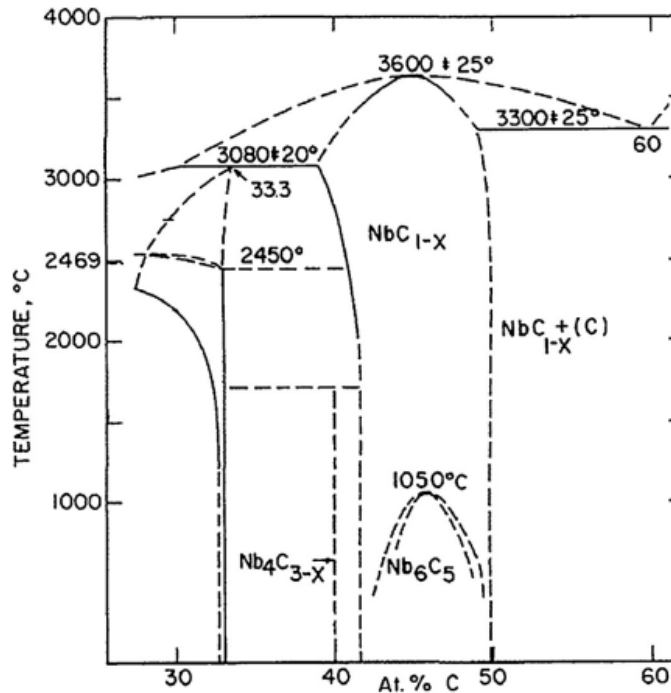
Figure 2.3: Binary phase diagram of Nb-C [24, 28]

The benefit of these sub-carbides is that mechanical properties like elastic modulus and hardness can be altered by the carbon stoichiometry in the range of 1 to 0.75 carbon. In this range, as the carbon content decreases, the lattice constant, elastic moduli, density, magnetic susceptibility and heat capacity also decreases. However, extensive increase in hardness is observed with the decrease in carbon content. It can be seen in figure 2.4 that in the range of 1 to 0.75 carbon content, the hardness increases and the values even exceeds the hardness of WC.

19
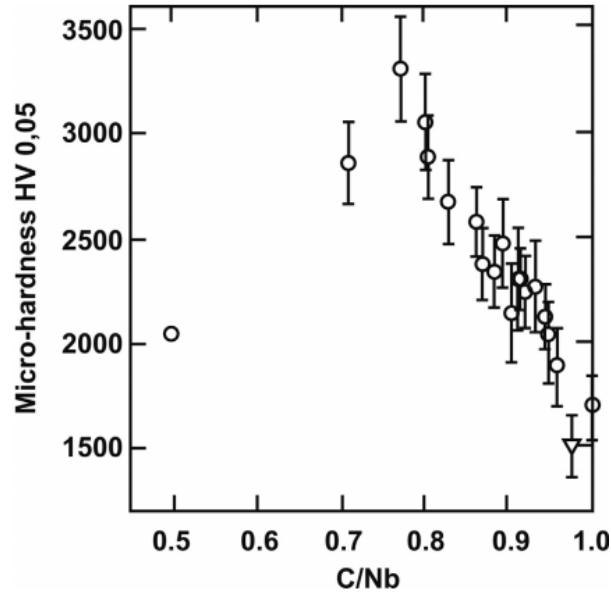
Figure 2.4: Micro-hardness vs Nb/C ratio variation [24]

2.2.2 Variation in binder

The table 2-3 tabulates the mechanical properties of NbC cermets with different metal binders. It can be visualized that Ni binder gives the maximum fracture toughness from them all. Also NbC12Ni showed higher flexural strength in comparison with NbC12Co cermet. The improved fracture toughness of NbC12Ni is because of its ductile Face Centered Cubic (FCC) structure available at all temperature. [29]

Table 2-3: Mechanical properties of NbC cermets with different binders

Sample	Hardness	Fracture toughness	Flexural strength	Reference
NbC12Ni	1130 ± 22	11.8 ± 0.4	---	[30]
NbC12(Ni30Al)	1360 ± 29	6.4 ± 0.2	---	
NbC12Co	1031 ± 7.1	7.27 ± 0.20	1010 ± 76	[29]
NbC12Ni	992 ± 11.22	14.73 ± 0.21	1379 ± 51	
NbC15(430L)	1387 ± 20.39	7.3 ± 0.4	---	[31]
NbC15(316L)	1275 ± 30.59	6.6 ± 0.5	---	

Sample				
NbC12Ni	1038 ± 26	10.6 ± 0.4	---	[32]
NbC12Co	1156 ± 11	7.2 ± 0.2	---	[33]

2.2.3 Effect of Secondary Carbides

Table 2-4 tabulates the mechanical properties variation after adding secondary carbide to NbC12Ni cermet.

Table 2-4: Mechanical properties of NbC12Ni cermets with different reinforcements

Sample	Hardness	Fracture toughness	Flexural strength	Reference
NbC12Ni4Mo$_2$C4VC4WC	1490 ± 15	9.2 ± 0.4	---	[30]
NbC12NixMo$_2$C	1198 ± 9.1	12.49 ± 0.18	1316 ± 32	[29]
NbC12NiyTiC	1093 ± 19.37	14.20 ± 0.11	1351 ± 9	
NbC12NixMo$_2$CyTiC	1301 ± 11.22	9.93 ± 0.14	1617 ± 22	
NbC12Ni4Mo$_2$C4VC	1301 ± 20.39	10.3 ± 0.3	1198	[34]
NbC12Ni5VC	1221 ± 2.0	11.7 ± 0.5	1222	
NbC12Ni10VC	1260 ± 14	9.7 ± 0.1	---	[32]
NbC12Ni5Mo$_2$C	1266 ± 13	9.0 ± 0.1	---	
NbC12Ni10Mo$_2$C	1369 ± 8	8.9 ± 0.1	---	

CHAPTER 3: EXPERIMENTATION METHODOLOGY

3.1   Fabrication process

Powder metallurgy route was used for fabrication of samples in this research work. The steps used in the fabrication are shown in the figure 3.1 and are discussed in detail in the following section.
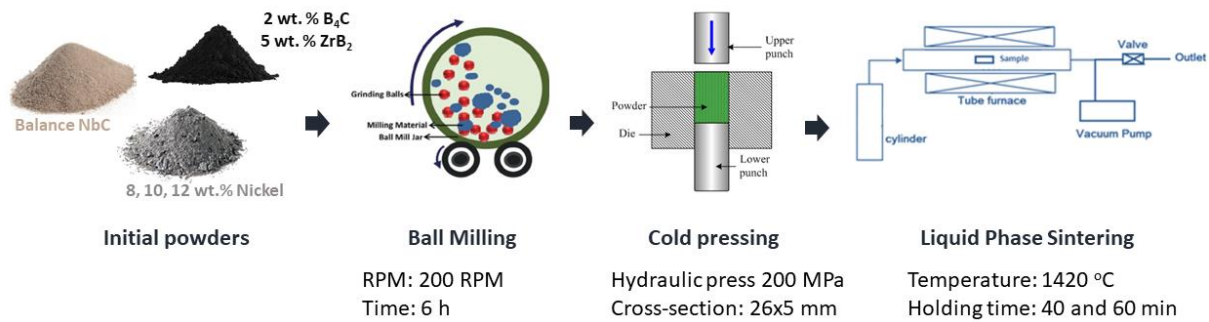
Figure 3.1: Schematic diagram of fabrication route

3.1.1   Powder mixing

Low energy ball milling machine was used for mixing of powders. Firstly, powders were weighed according to the wt.% shown in the table 3.1. Then these weighed powders were poured in a Polypropylene (PP) bottle along with steel ball in 1:10 proportion. These PP bottles were placed on ball mill shaft and then the machine was started by setting the RPM at 200. After 6 hours the ball mill was stopped and the mixed powder was extracted from the bottle.

3.1.2   Pressing

After mixing, the extracted powders were poured into a rectangular cross-sectioned die and placed under the hydraulic press to form rectangular pellets.

22

Table 3-1: List of samples and their composition

Processes	Samples	Powders composition, wt%				
		Ti	Ni	B4C	ZrB2	NbC
Binder variation	NbC8Ni	---	8	---	---	balance
	NbC10Ni	---	10	---	---	balance
	NbC12Ni	---	12	---	---	balance
Holding time variation	NbC12Ni5ZrB2(40 min)	---	12	---	0.5	balance
	NbC12Ni5ZrB2 (60 min)	---	12	---	0.5	balance
	NbC12Ni2B4C (40 min)	---	12	0.5	---	balance
	NbC12Ni2B4C (60 min)	---	12	0.5	---	balance
B₄C size variation	NbC12Ni2B4C (5um)	---	12	0.5	---	balance
	NbC12Ni2B4C (3um)	---	12	0.5	---	balance
Ti addition	NbC12Ni1.2Ti2B4C	1.2	12	0.5	---	balance

3.1.3 Sintering

These rectangular pellets were then placed in the furnace for sintering at 1420°C. To study the effect of holding time sintering was carried out at two different holding times i.e. 40 and 60 minutes.

3.2 Characterization

This section includes the working principal and process of the characterization techniques used for the evaluation of the samples. The characterization techniques discussed here are:

1. X-Ray Diffraction, XRD

2. Scanning Electron Microscopy, SEM

3. Density Measurement

4. Micro-Vickers

5. Single-Edge Notched Bending, SENB

6. Flexural testing

3.2.1 X-Ray Diffraction

XRD was used for the purity confirmation of the powder used for this research study. The principle of XRD is based on the phenomenon of X-ray-matter interaction as shown in figure 3.2. When X-rays fall on a surface they interact with the atomic planes in such a way that the scattering of the incident x-rays cancel in some directions and reinforce in others. The scattering will be detectable only when the x-rays are diffracted by same family of planes. The whole process is based on Bragg's Law i.e.

$$n\lambda = 2dSin\theta$$

Where,

d = spacing between the planes

n = integer representing order of diffraction

θ = diffraction angle

λ = wavelength of X-rays

The results of XRD ware obtained in the form of intensity Vs 2θ pattern which was then analyzed Xpert Highscore.
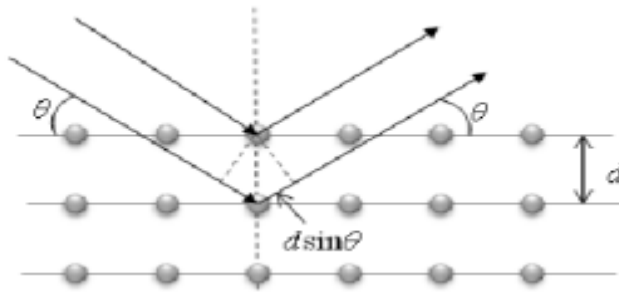
Figure 3.2 Diffraction from atomic planes

3.2.2   Scanning Electron Microscopy

SEM utilizes a beam of electrons in the range of 1eV to 1,000,000eV which is incident on the sample surface. This electron beam interacts in a variety of ways with the specimen surface which are:

a. Back Scattered Electrons
b. Secondary Electrons
c. Augers Electrons
d. Characteristic X-ray

These interactions depend directly on the penetration of the beam as depicted by figure 3.3 shown below:
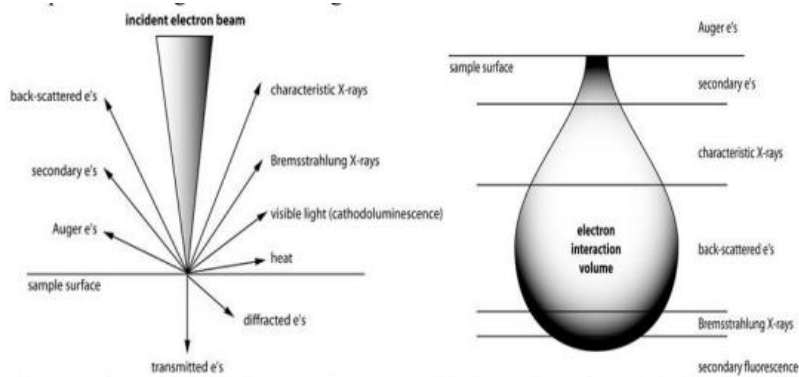

Figure 3.3 Electron Beam Interactions with Surface

For imaging secondary electrons are used in the process, these are generated due to the collision of incident electron beam with the outermost electrons of the surface atoms which are loosely bonded. The energy of secondary electrons depends directly on the energy of the incident beam and the depth range from which these electrons are emitted is between 2-50nm. These electrons are detected by the detector for imaging. The overall schematic of working mechanism of SEM is shown in figure 3.4.
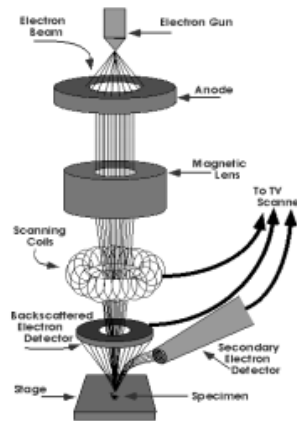
Figure 3.4 Working Mechanism of SEM

3.2.3   Density Measurement

Density of an unknown material is calculated using Archimedes principle which states that buoyant force that produces an upwards lift on an object under water, due to the pressure difference created below and above the object, is equal to the weight of water displaced or removed by that object submersed in water. This phenomenon is also used to calculate the volume of irregular shapes.

Figure 3.5: Density Measurement apparatus

Archimedes principle can be presented in the form of buoyant force (F_B) as:

$$F_B = \rho_f V_f g$$

Where,

ρ is density of fluid

V is volume of fluid

g is gravitational force

If the medium used for density calculations is water the density term can be avoided as the density of water is 1 kg/L and therefore the relation between force and volume can be exploited. The apparatus used for measure weight is shown below in Figure 3.5.

Sample is first weighed in air and the mass is called dry mass (W_{dry}) then it is suspended in a beaker of water and wet mass (W_{wet}) is measured. Thereafter density is calculated using the following formula:

$$density = \frac{W_{dry}}{W_{dry} - W_{wet}}$$

3.2.4 Micro-Vickers Hardness

Instead of using Rockwell, Brinnell, Vicker hardness tests, micro-Vickers was performed for hardness on all the samples because this technique precisely determines the hardness. The working principle of micro-Vickers technique is similar to that of Rockwell hardness testing i.e. an indent is made on the surface and then the dimensions of this indent are measured to determine the hardness of the surface. The indenter used in micro-Vickers is a diamond tip pyramidal indenter, which is used to make indents on the surface. Now harder the surface, smaller are the dimensions of indent and vice versa. The procedure used to measure hardness of the coating by us was:

a. Sample placement on micro-Vickers hardness tester
b. Setting of the apparatus to zero and image viewing through microscope
c. Application of load
d. Load removal and measurement of the dimensions of indent via optical microscope
e. Calculation of Vickers hardness number

Vickers hardness number is calculated on the basis of dimensions of the indent on the surface using following formula:

$$HV = \frac{2F sin\frac{136^o}{2}}{d^2} \qquad HV = 1.854\frac{F}{d^2}$$

Where:

HV= Vickers Hardness

d= Arithmetic mean of the two diagonals

F= Load in kgf

The schematic of the indenter is shown in figure 3.6, where the depth of the indent is usually 1/7th of diagonal length.
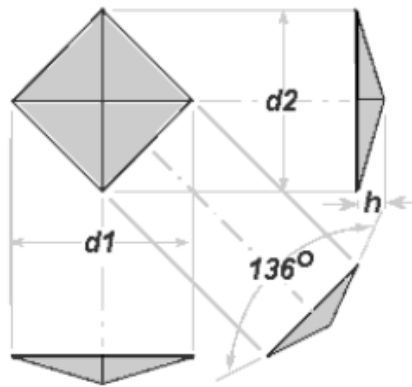

Figure 3.6 Schematic of Indenter

3.2.5   Fracture Toughness

In materials science, fracture toughness is the ability of material to sustain crack in order to avoid propagation of fracture and prevent failure. In other words, the ability of a defect or a flaw to cause fracture is determined by fracture toughness. Quantitatively it represents a materials property to resist brittle failure and is directly proportional to the energy absorbed during plastic deformation. Therefore, tougher materials are known to follow a more ductile fracture that is they underdo large plastic deformation before failure.
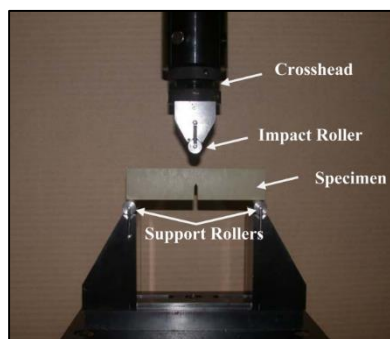

Figure 3.7: Fracture toughness assembly and sample

Fracture toughness is a function of energy required to cause fracture, stress applied and initial crack length and can be calculated as follows:

$$K_{IC} = \frac{3 \times P_{max} \times L}{2 \times b \times h^{3/2}} \times \alpha^{1/2} \times Y$$

Where,

$$Y = \frac{1.99 - \alpha(1-\alpha)(2.15 - 3.93\alpha + 2.7\alpha^2)}{(1+2\alpha)(1-\alpha)^{3/2}}$$

P_{max} = breaking load during three-point bending test,

L = bending span,

b = specimen width,

h = specimen height,

α = ratio between a (a is the notch depth) and h,

and Y = calibration factor

There are multiple ASTM standards that engineers use to prepare standardized samples for testing. Figure 3.7 represents the shape of specimen used in this study. The notch acts as an initial defect and stress concentration point where crack originates and propagates within the material. As mentioned earlier fracture toughness is the ability of material to sustain crack and is measured in terms of energy absorbed per unit area (KJ.m^{-2}).

CHAPTER 4: RESULTS AND DISCUSSION

4.1   Characterization of initial powders

4.1.1   Scanning electron microscopy

Figure 4.1 demonstrates the SEM images of initial powders used for this research. Fig 4.1 (a) shows NbC powder, its particle size varies from 0.1 – 4 um. However, amount of 4 um powder particle is very low and the major particle distribution lies between 0.1 – 1 um. Fig 4.1 (b) displays Ni powder, it is present in the form of a cluster, with a particle size of 1 um. Fig 4.1 (c) and (d) indicates particle size and morphology of B_4C powders. Both the powders confirm the same flaky morphology while particle size of (c) lies between 5 – 7 um whereas (d) lies between 1 – 3 um.
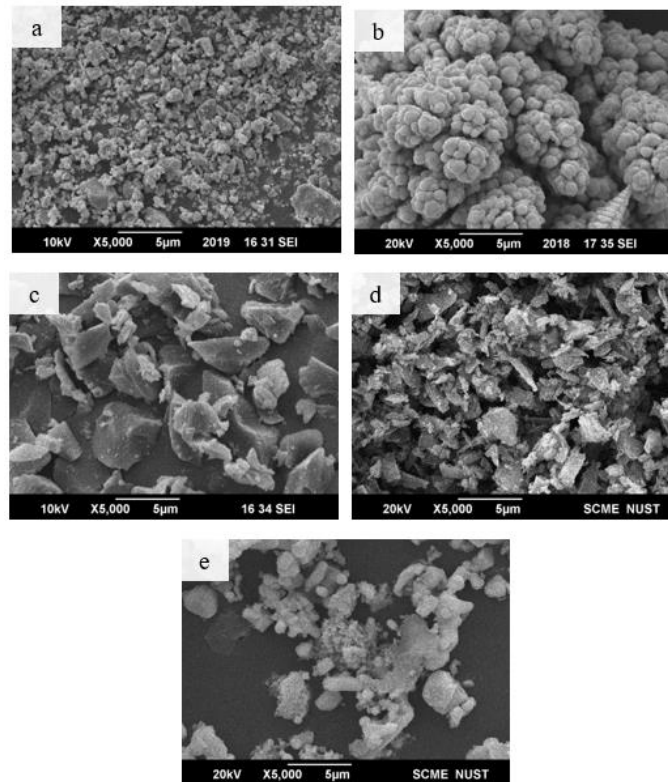

Figure 4.1: SEM image of (a) NbC, (b) Nickel, (c) B_4C (>5um), (d) B_4C (3um), (e) ZrB_2 powders

4.1.2 XRD of initial powders

Figure 4.2 shows the XRD patterns of pure powders used for further experimentation. Patterns of all the powders matches the standard and there was no extra peak to be found. The peaks correspond to pure powders showing no signs of impurities.
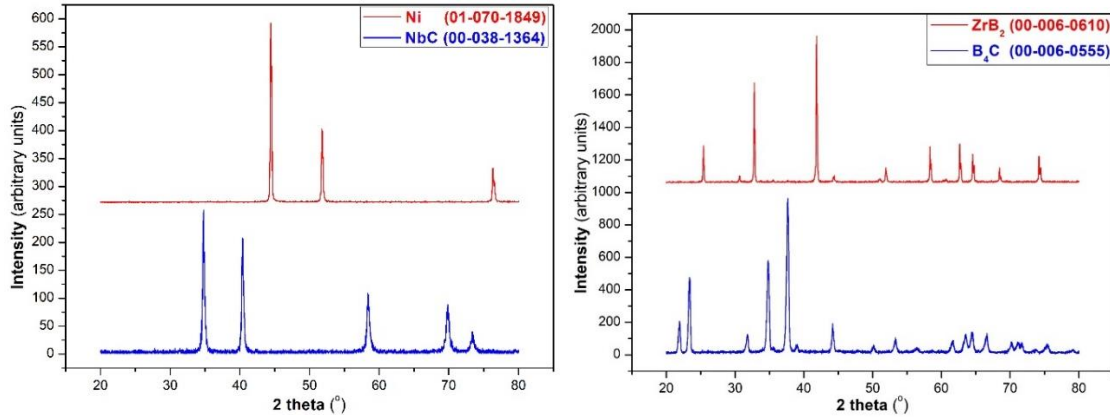

Figure 4.2: XRD pattern of initial powders

4.2   Characterization of binder variation

4.2.1   Scanning electron microscopy

Figure 4.3 illustrates the SEM images of sintered compacts, showing the effect of increase in binder concentration on the morphology and densification of the samples. It can be clearly observed that with the increase in binder composition from fig 4.3 (a) to (c) the porosity decreases. The increasing densification can be explained by the fact that with the increase in Nickel concentration the sufficient amount of nickel is available to infiltrate the pores, hence decreasing the porosity.
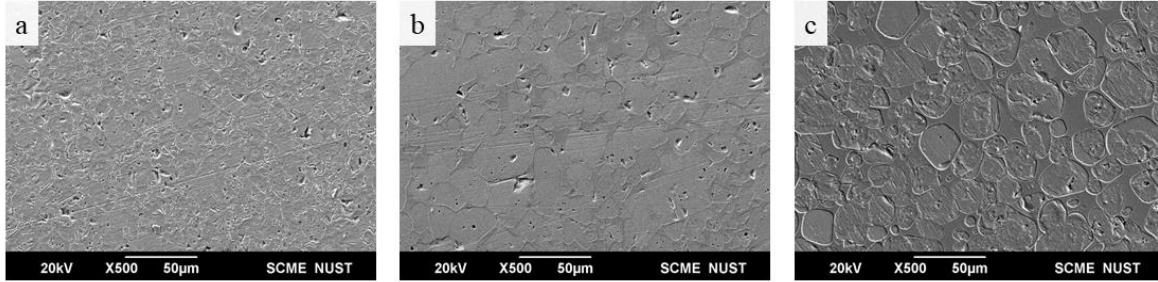
Figure 4.3: SEM images of (a) NbC8Ni, (b) NbC10Ni, (c) NbC12Ni

4.2.2 Mechanical Properties and Density

Figure 4.4 (a) shows that with increase in binder composition the flexural strength and percentage density increases. With increase in nickel composition the pores are filled, which improves densification. Pores, that act as stress concentration points, are the basic cause of crack initiation. Hence, reduction in porosity decreases the chances of crack initiation leading towards failure thus increasing the flexural strength. Moreover, nickel being a soft phase imparts toughness to the inherently brittle NbC phase.

Figure 4.4 (b) demonstrates an increase in fracture toughness and decrease in hardness with the increase in binder composition. Nickel being a soft phase, with FCC crystal structure, tends to decrease hardness whereas the fracture toughness increases because nickel is a tougher phase and increase in its amount increases the toughness of overall system.
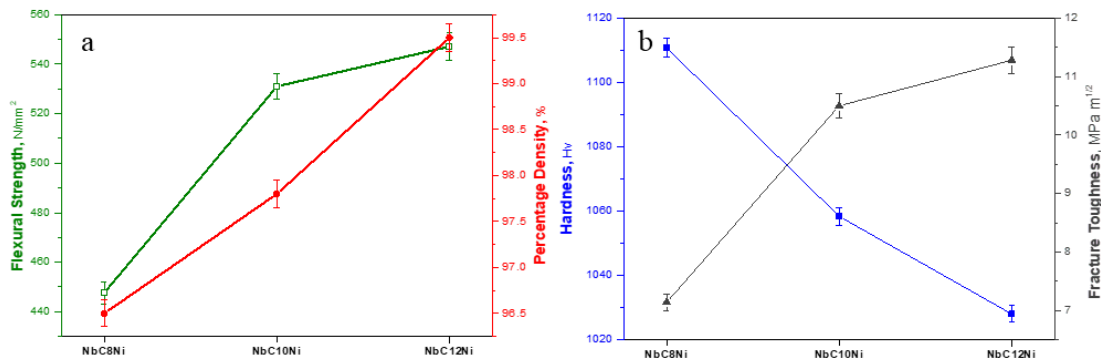

Figure 4.4: (a) Flexural strength and density (b) hardness and fracture toughness w.r.t binder concentration

33

Cermet with **12 wt. % Ni** demonstrated the maximum densification and hence the highest flexural strength and fracture toughness. Therefore, this system, after optimization, was selected for further study with the addition of reinforcements.

4.3 Effect of reinforcements

4.3.1 Scanning electron microscopy

Figure 4.5 show the micrographs of ZrB_2 and B_4C reinforced cermets of NbC with 12 wt.% Nickel as binder. It can be visualized that with the addition of reinforcement ZrB_2 and B_4C the porosity increases due to the tension created on the surface of reinforcement particles. This surface tension repels the nickel binder [35] and hence causing the creation of porosity. This surface tension can be reduced by either increasing the sintering temperature or holding time during sintering to provide sufficient time for diffusion. Another alternative could be the addition of metal binder which decreases this surface tension hence facilitating proper infiltration and reduction in porosity.
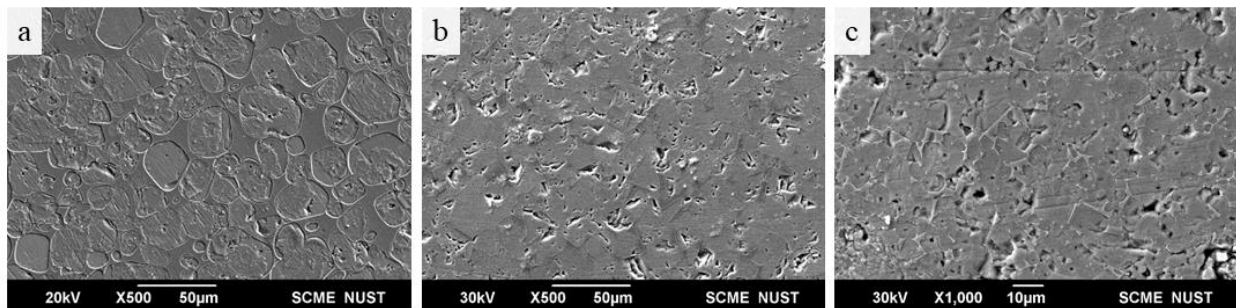

Figure 4.5: SEM images of (a) NbC12Ni, (b) NbC12Ni2B_4C and (c) NbC12Ni5ZrB_2

4.3.2 Mechanical Properties and Density

Figure 4.4 (a) displays that with addition of reinforcements the flexural strength and percentage density decrease. Decrease in densification increases the porosity which causes crack initiation and hence decreases the flexural strength. However, the hardness of the reinforced samples increases because the reinforcements have a superior hardness in comparison with the base carbide i.e. NbC.
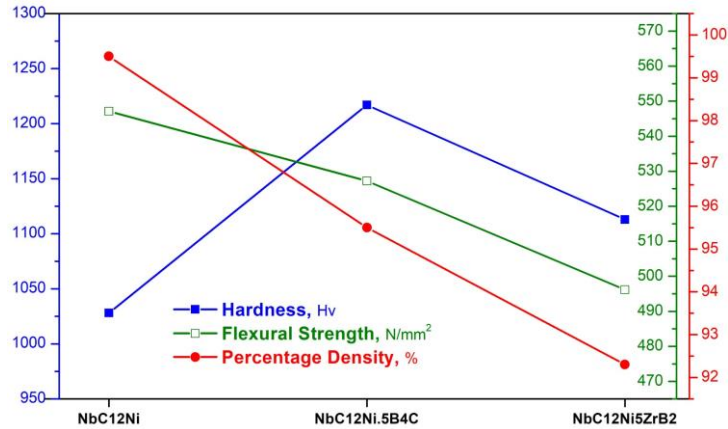
Figure 4.6: Mechanical properties and density graph

4.4 Effect of different particle size of B₄C reinforcements

4.4.1 Scanning electron microscopy

Figure 4.7 display the micrographs of effect of size variation of B₄C reinforcements in NbC 12 wt.% Nickel samples. It can be seen that with the decrease in particle size of B₄C from 5um to 3um the porosity increase even further. The decrease in particle size increases the overall surface area which increases the surface tension leading towards an increase in porosity due the repulsion of nickel hence resulting in lower densification.
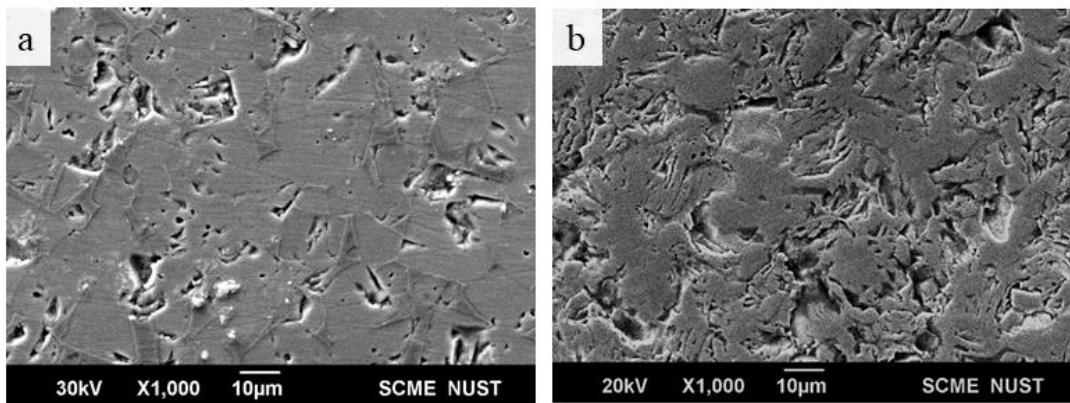

Figure 4.7: SEM images of NbC12Ni2B₄C samples with (a) 5um and (b) 3um particle size of B₄C

4.4.2 Mechanical Properties and Density

Figure 4.8 presents a bar graph to demonstrate the effect of B_4C reinforcements size in NbC12Ni cermets. The flexural strength and percentage density decrease with the decrease in particle size, but the hardness increases. The increase in hardness could be because of the increased amount of particles due to decrease in particle size.

As discussed earlier, due to the reduction in particle size and increase in surface tension, porosity increases with the decrease in particle size of B_4C reinforcements therefore resulting in a lower densification as shown in the bar chart below. High porosity leads towards lower flexural strength as pores serve as stress concentration points where cracks initiate, leading towards lower strength and failure. However, hardness increases with decrease in particle size despite of lower densification. This trend could be analyzed in terms of surface area and homogenous distribution of reinforcement particles, smaller particle size increases the surface area that means a number of particles are distributed evenly throughout the sample. In other words, percentage of B_4C particles per square centimeter would be higher comparatively. This distribution of smaller particles accounts for higher hardness in cermets with lower particles size of B_4C reinforcements. Moreover, hardness is known to be a surface property that is the porosity present in bulk samples would not directly affect the surface hardness.
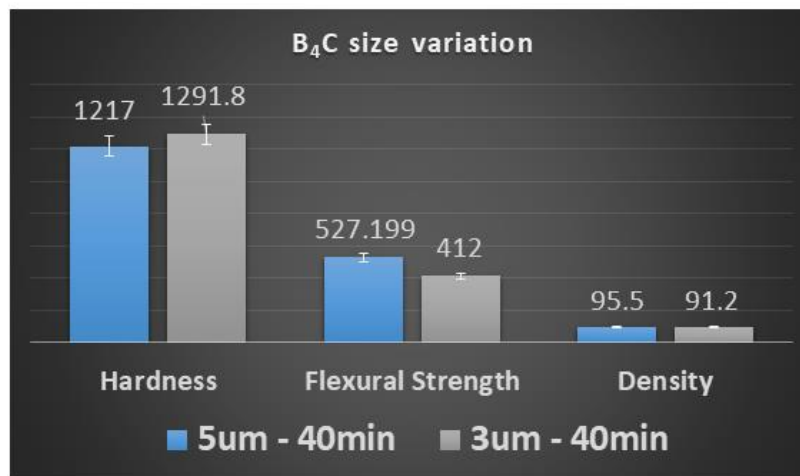

Figure 4.8: Mechanical properties and density graph

4.5   Effect of holding time

4.5.1   Scanning electron microscopy

Figure 4.9 illustrates the morphology of $NbC12Ni5ZrB_2$ and $NbC12Ni2B_4C$ cermets when sintered at $1420^{\circ}C$ with a holding time of 60 min. As compared to the previously sintered cermets with a holding time of 40 min, these compacts show a lower porosity and an increase in densification. This improved densification can be attributed to the diffusion mechanism during sintering where material diffuse through the grain boundaries and along the surface to fill the vacancies resulting in an overall densified structure. Increase in holding time at high temperatures allow sufficient time for diffusion to take place, that is nickel binder would have sufficient time to diffuse through and infiltrate the pores.
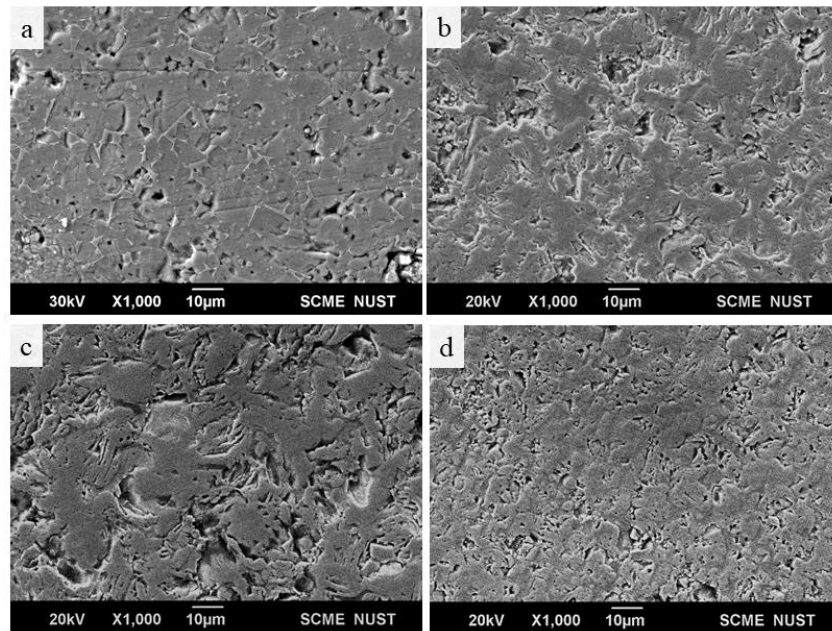

Figure 4.9: SEM images of holding time variation of $NbC12Ni5ZrB_2$ (a) 40 min, (b) 60 min and $NbC12Ni2B_4C$ (c) 40 min, (d) 60 min

4.5.2 Mechanical Properties and Density

Figure 4.10 demonstrates the mechanical properties and percentage density of NbC12Ni5ZrB$_2$ and NbC12Ni2B$_4$C cermets sintered for 40 and 60 minutes. In both the systems it can be observe that with increase in holding time the hardness decreases as increase in holding time increases grain size which decreases hardness. Whereas, flexural strength and percentage density increase as sufficient time is given for sintering which decreases the porosity and increases the flexural strength.
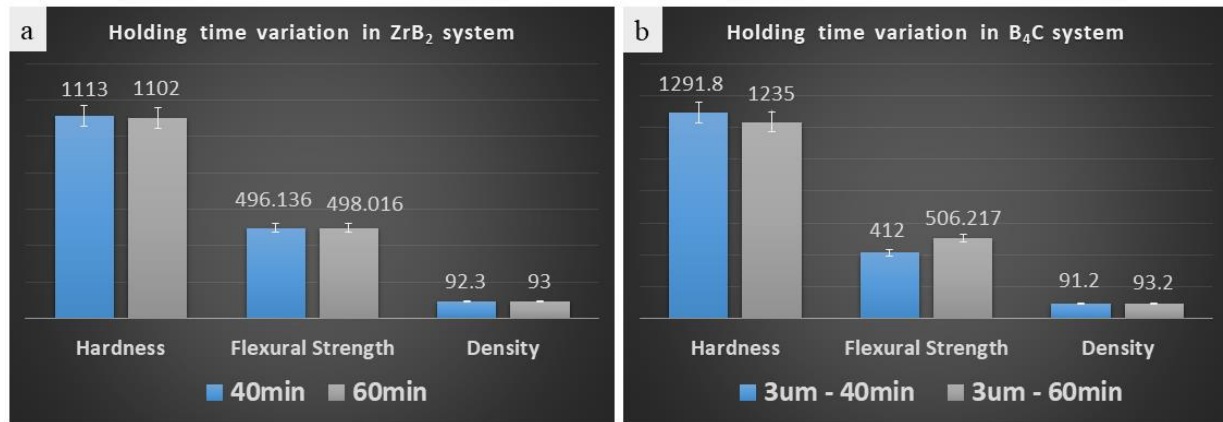

Figure 4.10: Mechanical properties vs density graphs of (a) ZrB$_2$ and (b) B$_4$C

4.6 Effect of titanium in B$_4$C system

4.6.1 Scanning electron microscopy

Figure 4.11 illustrates the morphology of NbC12Ni2B$_4$C cermets after addition of titanium which acts as a binder additive. Addition of titanium decreases porosity and improves densification as can be seen in the SEM image below, Figure 4.11 (b). Titanium was added to counter the effects of B$_4$C dissociation, as titanium is susceptible to TiB$_2$ formation. It is presumed that titanium reacts with boron on the interface of B$_4$C and Ni binder thereby decreasing surface energy and increasing wettability [36]. This facilitates liquid phase sintering mechanism and improving densification as nickel diffuse and infiltrate the pores.
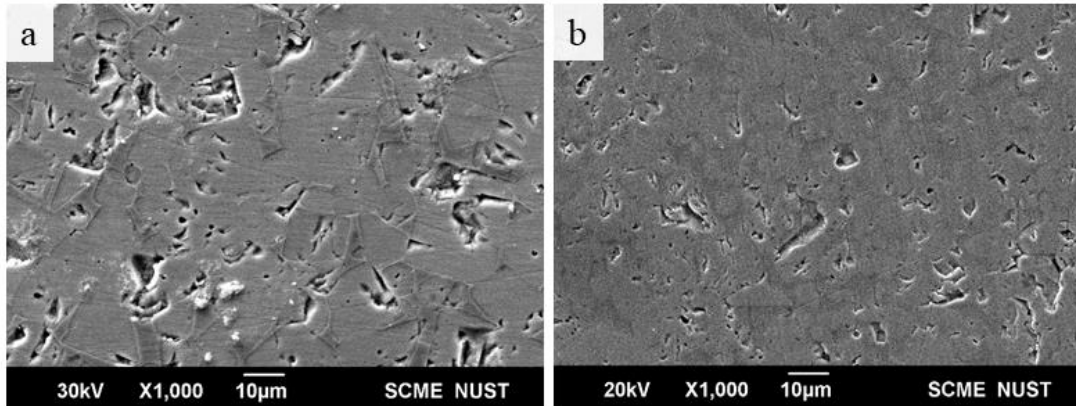
Figure 4.11: SEM images of (a) NbC12Ni2B$_4$C and (b) NbC12Ni1.2Ti2B4C

4.6.2 Mechanical Properties and Density

Figure 4.12 shows the bar graph comparison of mechanical properties and percentage density of NbC12Ni2B$_4$C and Titanium addition to this cermets. The addition of titanium to this system increases the hardness and percentage density because titanium reacts to form TiB$_2$ [37] on the interface of B$_4$C and Nickel [36]. This TiB$_2$ decreases the surface energies and increasing the wettability, hence improving the percentage density. Moreover, TiB$_2$ is a much harder than B$_4$C and NbC that's why hardness increases with a compromise in flexural strength.
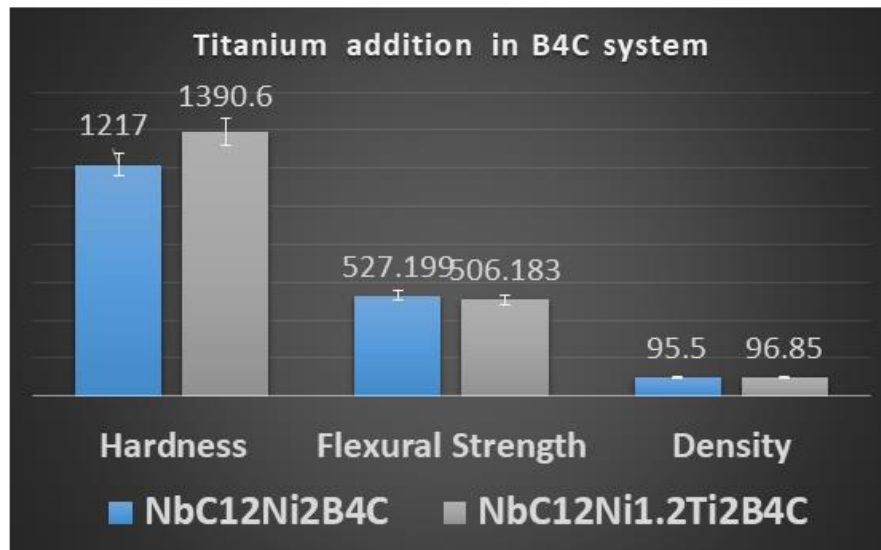
Figure 4.12: Mechanical properties and density graph

CONCLUSION

- NbC cermets with 12 % Nickel demonstrate the maximum densification, flexural strength and fracture toughness

- B_4C reinforcement gives superior properties in comparison with ZrB_2

- Smaller size of B_4C reinforcement demonstrate superior hardness with a compromise in densification

- Increase in holding time deteriorates the properties in both ZrB_2 and B_4C system

- Addition of titanium in B_4C system elevates the properties

FUTURE RECOMMENDATION

- This system can be further analyzed by varying the amount of reinforcement

- Study the effect of sintering temperatures

- Addition of other metal like Iron can be studied as a replacement of Titanium

REFERENCES

[1]   T. Enomoto, "Cermets," in *CIRP Encyclopedia of Production Engineering*, L. Laperrière and G. Reinhart, Eds., ed Berlin, Heidelberg: Springer Berlin Heidelberg, 2014, pp. 152-157.

[2]   A. Richter. (2018, 28-07-2021). *Cutting benefits of ceramic and cermet tools*. Available: https://www.ctemag.com/news/articles/cutting-benefits-ceramic-and-cermet-tools

[3]   K. TSUDA, "History of Development of Cemented Carbides and Cermet," *SEI Technical Reveiw,* 2016.

[4]   A. Aramian, S. M. J. Razavi, Z. Sadeghian, and F. Berto, "A review of additive manufacturing of cermets," *Additive Manufacturing,* vol. 33, p. 101130, 2020.

[5]   A. G. de la Obra, M. A. Avilés, Y. Torres, E. Chicardi, and F. J. Gotor, "A new family of cermets: Chemically complex but microstructurally simple," *International Journal of Refractory Metals and Hard Materials,* vol. 63, pp. 17-25, 2017.

[6]   A. Rajabi, M. J. Ghazali, J. Syarif, and A. R. Daud, "Development and application of tool wear: A review of the characterization of TiC-based cermets with different binders," *Chemical Engineering Journal,* vol. 255, pp. 445-452, 2014.

[7]   samaterials. (2018, 28-07-2021). *WHAT IS CERAMIC METAL?*

[8]   J. L.-H. Enrique Rocha-Rangel, Carlos A. Calles-Arriaga, Wilian J. Pech-Rodríguez, Eddie N. Armendáriz-Mireles, José A. Castillo-Robles and José A. Rodríguez-García, "Effect of additions of metal submicron particles on properties of alumina matrix composites," *Journal of Materials Research* vol. 34, pp. 2983-2989, 2019.

[9]   J. Kübarsepp and K. Juhani, "Cermets with Fe-alloy binder: A review," *International Journal of Refractory Metals and Hard Materials,* vol. 92, p. 105290, 2020.

[10]   T. F. Dietrich Munz, *Ceramics - Mechanical Properties, Failure Behaviour, Materials Selection*: Springer-Verlag Berlin Heidelberg, 1999.

[11]   B. G. Compton and F. W. Zok, "Impact resistance of TiC-based cermets," *International Journal of Impact Engineering,* vol. 62, pp. 75-87, 2013.

[12]   I. P. Borovinskaya, "Nitrides and Nitride Ceramics," pp. 214-218, 2017.

[13]   (28-07-2021). *Cermet Composite Powders*.

[14]   P. Ettmayer, "HARDMETALS AND CERMETS," *Annual Review of Materials Science,* vol. 19, pp. 145-164, 1989.

[15] W. L. P. Ettmayer, "The Story of Cermets," *International Journal of Powder Metallurgy,* vol. 21, pp. 37-38, April 1989.

[16] J. Meng, J. Lu, J. Wang, and S. Yang, "Tribological behavior of TiCN-based cermets at elevated temperatures," *Materials Science and Engineering: A,* vol. 418, pp. 68-76, 2006.

[17] I. Hussainova, "Some aspects of solid particle erosion of cermets," *Tribology International,* vol. 34, pp. 89-93, 2001.

[18] G. M. P. W. C. Oliver, "An improved technique for determining hardness and elastic modulus using load and displacement sensing indentation experiments," *Materials Research Society,* vol. 7, pp. 1564-1583, 31 January 1992.

[19] I. Hussainova, I. Jasiuk, M. Sardela, and M. Antonov, "Micromechanical properties and erosive wear performance of chromium carbide based cermets," *Wear,* vol. 267, pp. 152-159, 2009.

[20] K. Plucknett, "Cermets and Hardmetals," *Metals,* vol. 8, p. 963, 2018.

[21] R. M. German, P. Suri, and S. J. Park, "Review: liquid phase sintering," *Journal of Materials Science,* vol. 44, pp. 1-39, 2009/01/01 2009.

[22] D. Lison, "Chapter 34 - Cobalt," in *Handbook on the Toxicology of Metals (Fourth Edition)*, G. F. Nordberg, B. A. Fowler, and M. Nordberg, Eds., ed San Diego: Academic Press, 2015, pp. 743-763.

[23] J. García, V. Collado Ciprés, A. Blomqvist, and B. Kaplan, "Cemented carbide microstructures: a review," *International Journal of Refractory Metals and Hard Materials,* vol. 80, pp. 40-68, 2019/04/01 2019.

[24] M. Woydt, H. Mohrbacher, J. Vleugels, and S. Huang, "Niobium carbide for wear protection – tailoring its properties by processing and stoichiometry," *Metal Powder Report,* vol. 71, pp. 265-272, 2016.

[25] M. Braic, V. Braic, M. Balaceanu, A. Vladescu, C. N. Zoita, I. Titorencu*, et al.*, "Preparation and characterization of biocompatible Nb–C coatings," *Thin Solid Films,* vol. 519, pp. 4064-4068, 2011/04/01 2011.

[26] G. Ramírez, S. E. Rodil, H. Arzate, S. Muhl, and J. J. Olaya, "Niobium based coatings for dental implants," *Applied Surface Science,* vol. 257, pp. 2555-2559, 2011/01/15 2011.

[27] D. H. E. Uhlmann, K. Kropidlowksi, P. Meier, L. Prasol, M. Woydt, "Increased tool performance with niobium carbide based cutting materials in dry cylindrical turning," in *CIRP Conference on High Performance Cutting*, 2018, pp. 541-544.

[28]   M. Woydt, S. Huang, J. Vleugels, H. Mohrbacher, and E. Cannizza, "Potentials of niobium carbide (NbC) as cutting tools and for wear protection," *International Journal of Refractory Metals and Hard Materials,* vol. 72, pp. 380-387, 2018.

[29]   R. M. Genga, P. Rokebrand, L. A. Cornish, N. Nelwalani, G. Brandt, N. Kelling*, et al.*, "High-temperature sliding wear, elastic modulus and transverse rupture strength of Ni bonded NbC and WC cermets," *International Journal of Refractory Metals and Hard Materials,* vol. 87, p. 105143, 2020.

[30]   S. G. Huang, J. Vleugels, H. Mohrbacher, and M. Woydt, "Microstructure and mechanical properties of NbC matrix cermets using Ni containing metal binder," *Metal Powder Report,* vol. 71, pp. 349-355, 2016.

[31]   S. G. Huang, J. Vleugels, and H. Mohrbacher, "Stainless steel bonded NbC matrix cermets using a submicron NbC starting powder," *International Journal of Refractory Metals and Hard Materials,* vol. 63, pp. 26-31, 2017.

[32]   S. G. Huang, J. Vleugels, H. Mohrbacher, and M. Woydt, "NbC grain growth control and mechanical properties of Ni bonded NbC cermets prepared by vacuum liquid phase sintering," *International Journal of Refractory Metals and Hard Materials,* vol. 72, pp. 63-70, 2018.

[33]   S. G. Huang, K. Vanmeensel, H. Mohrbacher, M. Woydt, and J. Vleugels, "Microstructure and mechanical properties of NbC-matrix hardmetals with secondary carbide addition and different metal binders," *International Journal of Refractory Metals and Hard Materials,* vol. 48, pp. 418-426, 2015.

[34]   M. Woydt, S. Huang, E. Cannizza, J. Vleugels, and H. Mohrbacher, "Niobium carbide for machining and wear protection – Evolution of properties," *Metal Powder Report,* vol. 74, pp. 82-89, 2019.

[35]   Q. Lin and R. Sui, "Wetting of B4C by molten Ni at 1753K," *Journal of Alloys and Compounds,* vol. 556, pp. 274-279, 2013.

[36]   Q. Lin and R. Sui, "Wetting of B4C by molten Ni–Ti alloys at 1753K," *Journal of Alloys and Compounds,* vol. 577, pp. 37-43, 2013.

[37]   Y. F. Yang, H. Y. Wang, R. Y. Zhao, and Q. C. Jiang, "Effect of Reactant Particle Size on the Self-Propagating High-Temperature Synthesis Reaction Behaviors in the Ni-Ti-B4C System," *Metallurgical and Materials Transactions A,* vol. 40, pp. 232-239, 2008.